Available online at www.sciencedirect.com
SCIENCE DIRECT®
Journal of Nuclear Materials 321 (2003) 318–323
journal of nuclear materials
www.elsevier.com/locate/jnucmat

Gibbs energy of formation of the Rh–Te intermetallic compounds Rh_3Te_2 and $RhTe_{0.9}$

R. Mishra, M. Ali, S.R. Bharadwaj, D. Das *

Applied Chemistry Division, Bhabha Atomic Research Centre, Trombay, Mumbai 400085, India

Received 10 March 2003; accepted 9 June 2003

Abstract

The vaporization behavior of the intermetallic compounds Rh_3Te_2 and $RhTe_{0.9}$ was studied in the temperature range 1151–1234 and 1026–1092 K, respectively, by Knudsen effusion mass loss technique. The phase analysis of partially evaporated samples of Rh_3Te_2 (s) and $RhTe_{0.9}$ (s) together with the available information on Te bearing vapor species revealed that the compounds incongruently volatilize as Rh_3Te_2 (s) = 3Rh (s) + $2/n$Te$_n$ (g) and 3$RhTe_{0.9}$ (s) = Rh_3Te_2 (s) + $0.7/n$Te$_n$ (g), ($n = 1, 2$), respectively. The equilibrium vapor pressures of Te_2 (g) and Te (g) were derived from the total pressure $p(Te_n)$ measured over the mixtures Rh_3Te_2 (s) and Rh (s), and $RhTe_{0.9}$ (s) and Rh_3Te_2 (s) in the respective cases. The standard Gibbs energy of formation of Rh_3Te_2 and $RhTe_{0.9}$ derived using the above vapor pressure data and other auxiliary data could be expressed by the equations $\Delta_f G°(Rh_3Te_2, s)$ (kJ mol^{-1}) = $-176.9 + 0.039T \pm 7.0$ and $\Delta_f G°(RhTe_{0.9}, s)$ (kJ mol^{-1}) = $-74.7 + 0.015T \pm 3.0$ kJ mol^{-1}, respectively.

1. Introduction

A number of noble metals such as ruthenium, rhodium and palladium are formed in considerable amounts during the fission of ^{235}U and other fissile nuclides [1]. They remain alloyed in the irradiated fuel pins [2] of fast breeder reactors (FBR), pressurized heavy water reactors (PHWR) and boiling water reactors (BWR) in the different phases: (1) white inclusions, i.e. metallic precipitates containing Mo, Tc, Ru, Rh and Pd, (2) palladium intermetallic compounds and mixed phases containing Pd, Sn, Sb and Te, (3) plutonium containing compounds Pu $(Pd,In,Sn,Te)_{3+x}$ with high palladium content, (4) Pd–Ag–Cd precipitates. Tellurium, which is generated in moderate amounts in the nuclear fission remains distributed in the metallic phases. The volatile fission product achieves higher concentrations in the cooler regions where it has the tendency to segregate as intermetallic compounds with the noble metals [3,4]. Thermodynamic information on the noble-metal tellurides is important in the interpretation of the phase behavior of the metallic fission products and in the assessment of the vapor concentration of Te at the clad surface. The metalloid is known to corrode the stainless steel, or, Zircaloy clads [1]. Thermodynamic data of the tellurides are also useful in the assessment of Te release behavior into the environment under accidental conditions.

The phase diagram of the binary rhodium–tellurium system is available in the literature [5]. Seven known intermediate compounds with different crystal structures are reported [6–9]. But no information on the thermodynamic stability of these intermediate phases is available. The present paper deals with the determination of the Gibbs energy of formation of the rhodium rich compounds Rh_3Te_2 and $RhTe_{0.9}$ by employing the Knudsen effusion vapor pressure measurement technique.

2. Experimental

Powdered rhodium (Heraus, Hanau, and purity 99.9%) and tellurium (Aldrich Chem. Co., ≈60 mesh,

* Corresponding author. Tel.: +91-22 2559 5102; fax: +91-22 2550 5151.
E-mail address: dasd@apsara.barc.ernet.in (D. Das).

0022-3115/$ - see front matter © 2003 Elsevier B.V. All rights reserved.
doi:10.1016/S0022-3115(03)00301-5

and 99.999% purity) were used as the starting materials. Appropriate amounts of the powders were weighed, mixed thoroughly in an agate mortar and pressed into pellets in a steel die. The pellets containing 40 and 47.4 at.% Te were sealed in evacuated quartz ampoules and heated in a resistance furnace at temperatures of 1100 and 1025 K, respectively, for two weeks. A negligible amount of tellurium was seen sublimed onto the inner wall of the quartz ampoule. The samples were then characterized by chemical analysis, thermogravimetry (TG), differential thermal analysis (DTA) and X-ray diffraction methods (XRD). TG and DTA studies were done using a simultaneously recording TG–DTA instrument (SETARAM 92-16.18, France) at a heating rate of 10 K/min in pure argon atmosphere. X-ray powder diffraction studies were done using a Phillips X-ray diffractometer (Model PW-1820).

The thermodynamic stability of the compounds was determined by Knudsen effusion technique. In the present experiment the vapor pressure of Te was calculated from the total mass loss of the sample using a micro-thermobalance (SETARAM, Model B24). Fig. 1 gives the sketch diagram of the micro-thermobalance assembly. A cylindrical quartz cell of 14 mm diam., 20 mm height and with 0.97 mm diam. orifice at the center of the flat base was hung from the balance with a flexible platinum wire into the uniform temperature zone. The wall thickness at the orifice was about 0.94 mm. The effusion flux from the orifice was directed downwards with this arrangement. A quartz crucible (8 mm diam.) containing about 300 mg powdered sample was put over a quartz stand inside the cell. The ratio of the surface area of the sample to the orifice area was about 40. The cell was then closed with a quartz lid through lapped joint and the two parts were tightened together using a platinum wire. The Pt Pt-10%Rh thermocouple used for measuring the sample temperature was located about 1 mm away from the sample but well within the isothermal zone of the reaction tube. The whole system was closed in a vacuum-tight, imperviously recrystallized alumina tube of diameter 30 mm. The balance was attached to a high-vacuum system. An ultimate vacuum of 10^{-8} bar was achieved under dynamic conditions. A stability of ± 0.1 μg in the TG signal was achieved.

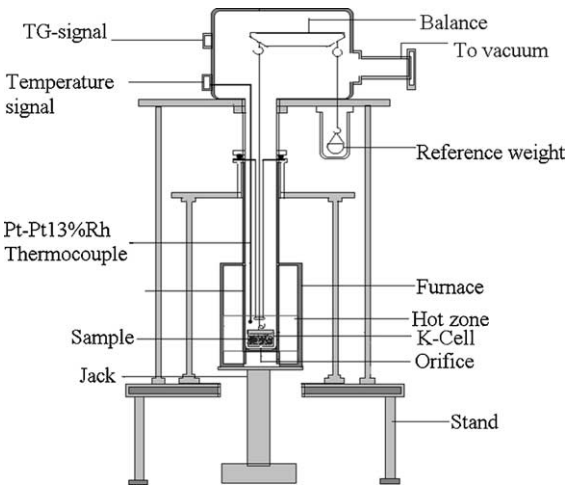

Fig. 1. Knudsen cell micro-thermobalance assembly.

The mass calibration of the microbalance was done using standard weights at room temperature. The temperature calibration for the sample was done by the drop method [10], using high purity metals such as In, Sn, Ag, Au etc. The observed melting point was 3 K less than the reported silver melting point (1235 K). Since the Ag-melting point falls within the temperature range of 1025–1235 K for this study, a correction of +3 K was applied in each temperature measurement.

The quartz Knudsen cell used in this study has a definite thickness of ≈0.94 mm and therefore, its Clausing factor had to be determined. It was determined by measuring the vapor pressure of some standard materials such as Ag (s), TeO_2 (s), $CdCl_2$ (s). The corresponding values of the factor were found to be 0.93, 0.947 and 0.961. The mean Clausing factor of 0.946 obtained from these data was used subsequently.

The mass loss from the Knudsen cell was monitored for the $Rh_3Te_2 + Rh$ and $RhTe_{0.9} + Rh_3Te_2$ two phase mixtures at different temperatures. The plots of the observed mass loss with respect to time in isothermal runs were used to calculate the vapor pressure. Mass loss measurements were taken at different temperatures in increasing as well as decreasing orders of successive isotherms. The observed reproducibility in the mass loss rate in each isothermal run confirms the absence of kinetic hindrance in the evaporative loss. Several measurements were carried out in the temperature range of 1151–1234 and 1026–1092 K for the two-phase $Rh_3Te_2 + Rh$ and $RhTe_{0.9} + Rh_3Te_2$ mixtures, respectively. The equilibrium vapor pressure derived from mass loss data in the respective systems was used to calculate the thermodynamic stability of Rh_3Te_2 and $RhTe_{0.9}$.

The residues in the silica crucible were analyzed after the experiments by X-ray diffraction to confirm the presence of the coexisting phases in the respective cases.

3. Results

3.1. Thermodynamic stability of Rh_3Te_2

Thermogravimetric and differential thermal analysis (TG–DTA) plot (Fig. 2) for the compound Rh_3Te_2 recorded under flowing argon conditions showed the onset of mass loss at about 1125 K before melting at 1260 K. XRD data for the residue of partially decomposed Rh_3Te_2 obtained from the Knudsen effusion studies

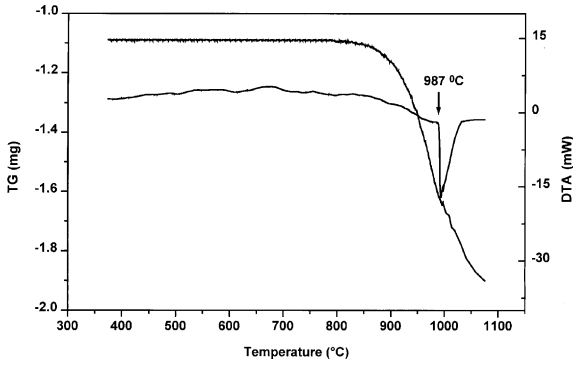

Fig. 2. TG–DTA plot for the compound Rh_3Te_2 recorded under flowing argon.

showed the presence of lines due to Rh and Rh_3Te_2 compounds in accordance with the phase diagram for the Rh–Te system [5]. From the available thermodynamic data [11] on tellurium bearing species at their total pressure of 10^{-7} bar in the experimental temperature range, it was observed that Te_2 (g) and Te (g) are the most predominant species. Therefore, the vaporization of Rh_3Te_2 during the effusion process was considered through the following reaction path

$$Rh_3Te_2\ (s) = 3Rh\ (s) + 2/nTe_n\ (g) \quad (n = 1, 2). \tag{1}$$

The rate of effusion of tellurium vapor from the orifice was obtained from the observed total mass loss under isothermal condition over a time t. The total vapor pressure of tellurium bearing species $p(Te_n)$, in the Knudsen cell was derived from the mass loss/time data using the relation obtained from kinetic theory of gases applied to the vapor fluxes of the two species, $f(Te)$ and $f(Te_2)$. The total mass loss, m_T within time t consists of m_{Te} and m_{Te_2}, respectively, due to mono and dimeric species of Te. The vapor pressures of the two species can be expressed in terms of the quantities m_{Te} and m_{Te_2} by the following relations:

$$p_i = (1/A) \times 1/K_c \times (m_i/t) \times (2\pi RT/M_i)^{1/2}, \tag{2}$$

where p_i is the vapor pressure of the ith species (i = Te, and Te_2), A the orifice area, K_c the Clausing factor, T the absolute temperature in K, M_i the molecular weight of the ith species, R the universal gas constant. Using Eq. (2) for the respective species and the fact that $m_T = m_{Te} + m_{Te_2}$, one arrives at a relation connecting the partial pressures of the two species with the observed mass loss as given below

$$p_{Te} + \sqrt{2}p_{Te_2} = (1/A) \times 1/K_c \times (m_T/t) \times (2\pi RT/M_{Te})^{1/2}. \tag{3}$$

The individual partial pressures, p_{Te} and p_{Te_2} were calculated using the above relation and the reported data [11] on the equilibrium constant of the reaction, Te_2 (g) = 2Te (g), expressed as $K = p_{Te}^2/p_{Te_2}$. Designating the left hand side of Eq. (3) as p_T, the vapor pressures of p_{Te_2} and p_{Te} can be expressed as

$$p_T = (K \times p_{Te_2})^{1/2} + \sqrt{2} \cdot p_{Te_2} \tag{4}$$

and

$$p_T = p_{Te} + \sqrt{2} \cdot p_{Te}^2/K. \tag{5}$$

The vapor pressure of Te (g), Te_2 (g) over the Rh_3Te_2 (s) and Rh (s) mixture in the temperature range 1151–1234 K as calculated from experimentally determined pa-

Table 1
Vaporization data for the reactions Rh_3Te_2 (s) = 3Rh (s) + Te_2 (g) and Rh_3Te_2 (s) = 3Rh (s) + 2Te (g)

Temperature (K)	Time, t (s)	Mass loss, w (μg)	$K^a \times 10^6$ (bar)	p_{Te} (Pa)	p_{Te_2} (Pa)
1151	300	30	0.9565	0.054	0.031
1160	300	38	1.1778	0.069	0.040
1169	300	48	1.4466	0.086	0.051
1179	300	61	1.8104	0.109	0.066
1182	300	68	1.9349	0.120	0.071
1187	500	119	2.1605	0.129	0.077
1194	600	165	2.5171	0.149	0.089
1199	300	95	2.8041	0.171	0.104
1200	600	195	2.8649	0.175	0.107
1202	900	337	2.9903	0.195	0.128
1205	500	191	3.1881	0.202	0.128
1209	500	202	3.4709	0.216	0.135
1211	300	134	3.6206	0.235	0.152
1219	300	147	4.2812	0.264	0.163
1226	500	302	4.9482	0.320	0.207
1234	300	203	5.8273	0.365	0.228

[a] $K = p_{Te}^2/p_{Te_2}$.

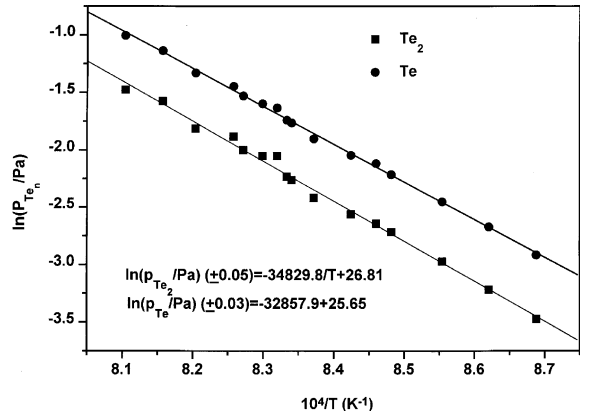

Fig. 3. $\ln(p_{Te_2}/Pa)$ and $(\ln p_{Te}/Pa)$ versus reciprocal temperature for the reactions Rh_3Te_2 (s) = 3Rh (s) + Te_2 (g) and Rh_3Te_2 (s) = 3Rh (s) + 2Te (g).

rameters involved in Eq. (3) and the equilibrium constant K in (4), (5), respectively, are given in Table 1 for all the runs. The linear least-square fits for $\ln p_{Te_2}$, and $\ln p_{Te}$ versus $1/T$ are given in Fig. 3. The least-square fitted equations are represented as

$$\ln(p_{Te_2}/Pa) = -34\,829.8/T + 26.8 \pm 0.05 \quad (1151 \leqslant T/K \leqslant 1234), \tag{6}$$

$$\ln(p_{Te}/Pa) = -32\,859.0/T + 25.7 \pm 0.03 \quad (1151 \leqslant T/K \leqslant 1234). \tag{7}$$

The slope and the intercept of the linear equations yield the values of enthalpy and entropy, respectively, averaged over the working range of temperatures for the incongruent vaporization of Rh_3Te_2 represented in Eq. (1). These values of enthalpy and entropy for vaporization of Te_2 (g) are (289.6 ± 6.4) kJ mol^{-1} and (127.0 ± 5.4) J K^{-1} mol^{-1}, respectively and that of Te (g) are (546.4 ± 7.0) kJ mol^{-1} and (235.0 ± 6.0) J K^{-1} mol^{-1}, respectively.

The Gibbs energy of formation of Rh_3Te_2 was derived using the above the vapor pressure data. In the derivation of the Gibbs energy of formation of Rh_3Te_2, it was assumed that the Rh_3Te_2 phase co-exists with pure Rh (s), as there is negligible Te solubility in Rh (s) [5]. Further, since the compound Rh_3Te_2 has a very narrow homogeneity range (<0.1 mol%) [5], it was considered as a line compound for the derivation. The vapor pressure data (Eqs. (6) and (7)) were therefore used in conjunction with the Gibbs energy of formation of Rh (s), Te (g) and Te_2 (g), to derive $\Delta_f G^\circ$ of Rh_3Te_2 (s).

The value of the Gibbs energy of formation of pure Rh (s) is taken as zero. The values of the Gibbs energy of formation of Te (g) and Te_2 (g) were taken from Ref. [12]. The Gibbs energy of formation of Rh_3Te_2 (s) thus can be expressed by the equations

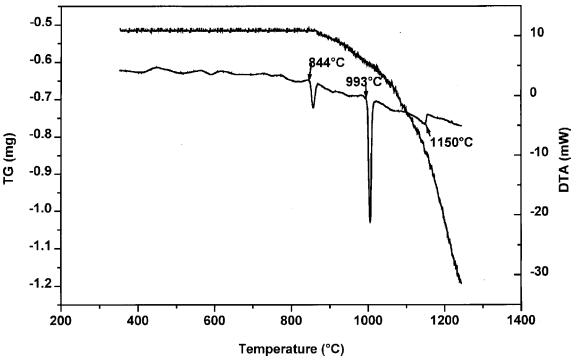

Fig. 4. TG–DTA plot for the compound $RhTe_{0.9}$ recorded under flowing argon.

$$\Delta_f G^\circ(Rh_3Te_2, s)\ (kJ\,mol^{-1}) = -175.0 + 0.037T \pm 7.0 \quad (1151 \leqslant T/K \leqslant 1234), \tag{8}$$

$$\Delta_f G^\circ(Rh_3Te_2, s)\ (kJ\,mol^{-1}) = -178.8 + 0.041T \pm 6.0 \quad (1151 \leqslant T/K \leqslant 1234). \tag{9}$$

Therefore, the average standard enthalpy and entropy of formation of Rh_3Te_2 at the mean temperature of measurement are $-(176.9 \pm 7.0)$ kJ mol^{-1} and $-(39.0 \pm 6.0)$ J K^{-1} mol^{-1} respectively.

3.2. Thermodynamic stability of $RhTe_{0.9}$

The TG–DTA plot for the compound $RhTe_{0.9}$ (Fig. 4) showed a slight mass loss before it decomposed into Rh_3Te_2 (s) and Rh_3Te_4 (s) at 844 °C. This peritectic decomposition has been reported to take place at 829 °C [5]. The Knudsen effusion measurement of the compound $RhTe_{0.9}$ was therefore carried out in the temperature range of 1026–1092 K, which is below the peritectic decomposition temperature of the compound mentioned above. The XRD data of partially decomposed $RhTe_{0.9}$ obtained at the end of the Knudsen effusion measurements showed the presence of lines due to Rh_3Te_2 and $RhTe_{0.9}$ compounds in accordance with the phase diagram [5]. Similar to the Rh_3Te_2 compound, in this case also Te (g) and Te_2 (g) are the most predominant tellurium bearing vapor species in the temperature range of measurement and Te bearing vapor pressure in the range of 10^{-8} bar. Therefore, the vaporization of $RhTe_{0.9}$ during the effusion was mostly through the following reaction path:

$$3RhTe_{0.9}\ (s) = Rh_3Te_2\ (s) + 0.7/nTe_n\ (g) \quad (n = 1, 2). \tag{10}$$

The rate of effusion of tellurium bearing species from the orifice was obtained from the total mass loss recorded

Table 2
Vaporization data for the reactions $3RhTe_{0.9}$ (s) = Rh_3Te_2 (s) + 0.35Te_2 (g) and $3RhTe_{0.9}$ (s) = Rh_3Te_2 (s) + 0.70Te (g)

Temperature (K)	Time, t (s)	Mass loss (w) (μg)	$K^a \times 10^7$ (bar)	p_{Te} (Pa)	p_{Te_2} (Pa)
1026	3000	32	0.3614	0.0039	0.0042
1030	3000	39	0.4064	0.0046	0.0053
1035	2350	29	0.4699	0.0047	0.0048
1039	2000	30	0.5273	0.0056	0.0059
1049	1200	24	0.7005	0.0075	0.0080
1053	1680	36	0.7836	0.0081	0.0085
1063	1170	32	1.0331	0.0106	0.0108
1072	840	30	1.3192	0.0137	0.0142
1074	1200	46	1.3921	0.0146	0.0154
1079	1200	50	1.5909	0.0162	0.0165
1082	880	39	1.7226	0.0174	0.0175
1084	600	30	1.8159	0.0192	0.0202
1087	600	33	1.9647	0.0209	0.0223
1092	600	37	2.2383	0.0236	0.0250

[a] $K = p_{Te}^2/p_{Te_2}$.

using the micro-thermobalance over a time t. The partial pressure of Te-dimer in the Knudsen cell was calculated from the mass loss/time data using the relations (3)–(5). The vapor pressure of Te (g) and Te_2 (g) over $RhTe_{0.9}$ in the temperature range of 1026–1092 K so derived is given in Table 2 for all the runs. The linear least-square fit of $\ln p_{Te}$ and $\ln p_{Te_2}$ versus $1/T$ for the experimental results is given in Fig. 5. The least-square fitted equations are represented as

$$\ln(p_{Te_2}/\mathrm{Pa}) = -29\,698.0/T + 23.5 \pm 0.06 \quad (1026 \leqslant T/K \leqslant 1092), \tag{11}$$

$$\ln(p_{Te}/\mathrm{Pa}) = -30\,400.4/T + 24.1 \pm 0.03 \quad (1026 \leqslant T/K \leqslant 1092). \tag{12}$$

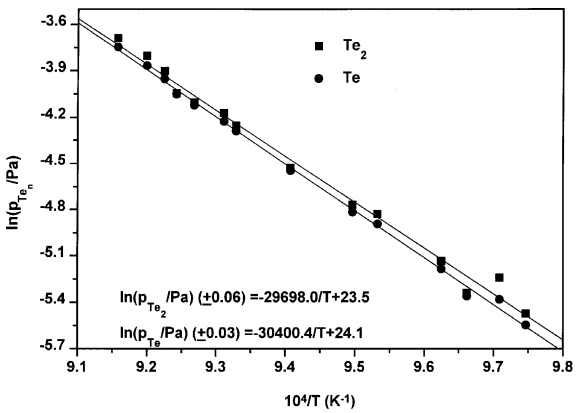

Fig. 5. $\ln(p_{Te_2}/\mathrm{Pa})$ and $\ln(p_{Te}/\mathrm{Pa})$ versus reciprocal temperature for the reactions $3RhTe_{0.9}$ (s) = Rh_3Te_2 (s) + 0.35Te_2 (g) and $3RhTe_{0.9}$ (s) = Rh_3Te_2 (s) + 0.70Te (g).

Slope and intercept of the linear equations yield the values of enthalpy and entropy, respectively, averaged over the working range of temperatures for the incongruent vaporization of $RhTe_{0.9}$ represented in Eq. (10). These values of enthalpy and entropy for vaporization of Te_2 (g) are (28.9 ± 0.8) kJ mol^{-1} and (11.6 ± 0.7) J K^{-1} mol^{-1}, respectively, and that of Te (g) are $(58.9 \pm 0.8$ kJ mol^{-1} and (24.3 ± 0.8) J K^{-1} mol^{-1}, respectively.

The Gibbs energy of formation of $RhTe_{0.9}$ was derived using the vapor pressure data of Te_2 (g) and Te (g) measured over the two-phase mixture Rh_3Te_2 (s) and $RhTe_{0.9}$ (s) in the temperature range 1026–1092 K. To derive the value of $\Delta_f G°$ of $RhTe_{0.9}$ (s), the vapor pressure data (Eqs. (11) and (12)) were used in conjunction with the Gibbs energy of formation of Te (g) and Te_2 (g) [12], and that of the co-existing phase Rh_3Te_2 (s) given by the average of Eqs. (8) and (9). The Gibbs energy of formation of $RhTe_{0.9}$ so obtained could be expressed by

$$\Delta_f G°(RhTe_{0.9}, s)\ (\mathrm{kJ\,mol^{-1}}) = -75.0 + 0.015T \pm 3.0 \quad (1026 \leqslant T/K \leqslant 1092), \tag{13}$$

$$\Delta_f G°(RhTe_{0.9}, \mathrm{s})\ (\mathrm{kJ\,mol^{-1}}) = -74.5 + 0.014T \pm 3.0 \quad (1026 \leqslant T/K \leqslant 1092). \tag{14}$$

The average standard enthalpy and entropy of formation of $RhTe_{0.9}$ at the mean temperature of measurement are therefore $-(74.7 \pm 3.0)$ kJ mol^{-1} and $-(15 \pm 3.0)$ J K^{-1} mol^{-1}, respectively.

4. Discussion

The derived data of the Gibbs energy of formation of Rh_3Te_2 (s) and $RhTe_{0.9}$ (s) were used to assess the

stability of the third intermetallic phase Rh_3Te_4 (s) which was found to be formed by the peritectic decomposition of $RhTe_{0.9}$ (s) as observed in the TG–DTA analysis. As the compound decomposes at 1117 K according to the reaction

$$RhTe_{0.9}\ (s) = 0.217Rh_3Te_2\ (s) + 0.117Rh_3Te_4\ (s), \tag{15}$$

the Gibbs energy of formation of Rh_3Te_4 (s) can be expressed as

$$\Delta_f G^\circ(Rh_3Te_4, s) \geqslant 8.547\Delta_f G^\circ(RhTe_{0.9}, s) - 1.855\Delta_f G^\circ(Rh_3Te_2, s) \quad \text{for } T \leqslant 1117 \text{ K}.$$

Considering this and making use of the values of $\Delta_f G^\circ(Rh_3Te_2, s)$ and $\Delta_f G^\circ(RhTe_{0.9}, s)$ derived from the average values of enthalpies and entropies of Eqs. ((8) and (9)) and ((13) and (14)), respectively, the Gibbs energy of formation of Rh_3Te_4 (s) works out to be $\Delta_f G^\circ(Rh_3Te_4, s) \geqslant -310.3 + 0.055T$ kJ mol^{-1} for $T \leqslant 1117$ K. The peritectic decomposition suggests that the ΔH° and ΔS° values of reaction (15) are positive. These restrictions on enthalpy and entropy values of the reaction (15) lead to $\Delta_f H^\circ(Rh_3Te_4, s) > -310.3$ kJ mol^{-1} and $\Delta_f S^\circ(Rh_3Te_4, s) > -55$ J K^{-1} mol^{-1}.

The excess entropy per mole of Rh for Rh_3Te_2 and $RhTe_{0.9}$ from this work was calculated to be −13 and −15 J K^{-1} mol^{-1}, respectively, at 1100 K. Assuming the same excess entropy for Rh_3Te_4, the estimated entropy for this compound at 1100 K works out to be 610 J K^{-1} mol^{-1}. The value of entropy of formation of Rh_3Te_4 at 1100 K, with this estimated S°_{1100} is −42 J K^{-1} mol^{-1}. This agrees with the prediction that $\Delta_f S^\circ(Rh_3Te_4, s) > -55$ J K^{-1} mol^{-1} made in the previous paragraph. Using this value of the entropy of formation, ($\Delta_f S^\circ$), and the fact that $RhTe_{0.9}$ decomposes peritectically according to Eq. (15), the enthalpy of formation of Rh_3Te_4 at 1100 K can be estimated to be −301 kJ mol^{-1} which again is in agreement with the inequality derived in the previous paragraph, viz. $\Delta_f H^\circ(Rh_3Te_4, s) > -310.3$ kJ mol^{-1} for temperatures $T \leqslant 1117$ K.

5. Conclusion

The Gibbs energies of formation of Rh_3Te_2 and $RhTe_{0.9}$ in the temperature ranges 1151–1234 and 1026–1092 K, respectively, derived from the vapor pressure data and Gibbs energy of formation data of Te_2 (g) and Te (g) could be expressed by the equations $\Delta_f G^\circ(Rh_3Te_2, s)$ (kJ mol^{-1}) $= -176.9 + 0.039T \pm 7.0$ and $\Delta_f G^\circ(RhTe_{0.9}, s)$ (kJ mol^{-1}) $= -74.7 + 0.015T \pm 3.0$.

Acknowledgements

The authors thank Mr A.N. Shirsat and Mr A.S. Kerkar for their help during the design and fabrication of the apparatus. They also thank Dr J.P. Mittal, Director, Chemistry and Isotope Group, BARC and Dr N.M. Gupta, Head, Applied Chemistry Division, BARC for their support and interest in this work.

References

[1] H. Kleykamp, J. Nucl. Mater. 131 (1985) 221.
[2] J.I. Bramman, R.M. Sharpe, D. Thron, G. Yates, J. Nucl. Mater. 25 (1968) 201.
[3] A.A. Men'kov, L.N. Komissarova, Yu.P. Simanov, V.I. Spitsyn, Dokl. Akad. Nauk SSSR 141 (1961) 3642.
[4] J.H. Brixner, J. Inorg. Nucl. Chem. 15 (1960) 199.
[5] Zh. Ding, H. Kleykamp, F. Thümmler, J. Nucl. Mater. 171 (1990) 134.
[6] W.H. Zachariasen, Acta Cryst. 20 (1966) 334.
[7] S. Geller, J. Am. Chem. Soc. 77 (1955) 2641.
[8] R.H. Plovnik, A. Wold, Inorg. Chem. 7 (1968) 2596.
[9] A. Kjekshus, T. Rakke, A.F. Andersen, Acta Chem. Scand. A 32 (1978) 209.
[10] O. Kubaschewski, C.B. Alcock, P.J. Spencer, Metallurgical Thermochemistry, 6th Ed., Pergamon, Oxford, 1993.
[11] FACTSAGE™ 5.0. Thermochemical Software for Windows™. Obtained from GTT Technologies, Germany, 2001.
[12] E.H.P. Cordfunke, R.J.M. Konings (Eds.), Thermochemical Data for Reactor Materials and Fission Products, North Holland, Amsterdam, 1990.